Inverse Problems in Engineering: Theory and Practice
3rd Int. Conference on Inverse Problems in Engineering
June 13-18, 1999, Port Ludlow, WA, USA

3ICIPE99/ID12

NONLINEARITY, SCALE, AND SENSITIVITY FOR PARAMETER ESTIMATION PROBLEMS: SOME IMPLICATIONS FOR ERROR ANALYSIS

Trond Mannseth*
Reservoir Department
RF-Rogaland Research
Thormøhlensgt. 55
N-5008 Bergen, Norway
Email: trond.mannseth@rf.no

Alv-Arne Grimstad†
Department of Physics
University of Bergen
Allégt. 55
N-5007 Bergen, Norway

Kristofer Kolltveit
Department of Physics
University of Bergen
Allégt. 55
N-5007 Bergen, Norway
Email: kristofer.kolltveit@fi.uib.no

Jan-Erik Nordtvedt
Reservoir Department
RF-Rogaland Research
Thormøhlensgt. 55
N-5008 Bergen, Norway
Email: jan-erik.nordtvedt@rf.no

ABSTRACT

Uncertainty assessment for parameter estimation problems is considered. It is customary to use confidence regions or intervals to give the precision of the parameter estimates. The method most used, because of modest computational requirements, is linearized covariance analysis.

Monte Carlo analysis can be used to check the validity of the linearization for a particular model, but is clearly not practical as a standard procedure. Curvature measures of nonlinearity have been suggested as a diagnostic tool to help decide when the linearized analysis is applicable.

For an ODE model, a correlation between high nonlinearity, low sensitivity, and small-scale perturbations, has been reported. Recently, the existence of such a correlation for a large class of nonlinear models, including the ODE model, was found.

Here, we utilize this correlation within assessment of parameter uncertainty. It is shown that care must be exercised when applying nonlinearity measures as a diagnostic tool for the validity of linearized covariance analysis. For models within the class where the correlation applies, a modified version of the nonlinearity measures may be preferable for this purpose.

1 INTRODUCTION

An important part of nonlinear parameter identification is to assess the accuracy of the estimated parameters. The most commonly used method, linearized covariance analysis (LCA), see e.g. (Seber and Wild, 1989), is only approximate for nonlinear models.

Several attempts have been made to construct reliable measures that are capable of predicting when the approximate methods will be inadequate. The measures of (Bates and Watts, 1980) employ differential geometry to calculate a measure of the curvature of the model at a point in parameter space. Critical values of the curvature measures, above which linearization methods may be significantly wrong, are given, based on considerations on the shape of linearized confidence regions.

*Address all correspondence to this author.
†Now with RF-Rogaland Research, Thormøhlensgt. 55, N-5008 Bergen, Norway, Email: alv-arne.grimstad@rf.no

Copyright © 1999 by ASME

Calibration of the proposed measures has to be done by numerical tests. In (Donaldson and Schnabel, 1987) an extensive evaluation of a series of different models was performed, using Monte Carlo (MC) simulations. They checked the predictions of several methods to calculate confidence regions. The recommended curvature limits of (Bates and Watts, 1980) were found to give good indications as to when the linearization methods were insufficient. It was found that LCA produced confidence regions with actual coverage far below the nominal confidence level when the maximum curvature values exceeded the Bates and Watts cutoff levels.

Attempts (Sylte et al., 1999) to employ the curvature measures to validate LCA predictions for a porous-media flow model, using MC simulations, produced results in apparent conflict with the results of Donaldson and Schnabel. High values of the curvature measure were observed together with conservative confidence intervals for the parameters. Wide confidence intervals corresponds to low sensitivity. A correlation between high curvature and low sensitivity was observed in a study of an ODE model (Chavent and Liu, 1989; Liu, 1993), and was coupled to the length scale of the basis elements in a multi scale representation of the unknown function.

Such a correlation was found to be valid for a class of models including the ODE model in (Chavent and Liu, 1989; Liu, 1993), under certain conditions (Grimstad and Mannseth, 1999). There are indications that the class may be extended to include also the PDE model studied in (Sylte et al., 1999), but due to the complexity of this model, such an extension may not be verified analytically. The case may only be made probable by numerical experiments.

The models of (Donaldson and Schnabel, 1987) are not included in the model class of (Grimstad and Mannseth, 1999), and this may be the reason for the different behavior with respect to nonlinearity and coverage.

The model in (Sylte et al., 1999) is such that the available data may not always be sufficient to determine the functions to be estimated well on the entire interval of definition. This means that there often occur parameter combinations that have associated low sensitivity. If a correlation like the one seen in (Grimstad and Mannseth, 1999) is also valid for the model in (Sylte et al., 1999), one would observe the highest curvature for these parameter combinations. Thus, LCA coverage may be high in regions where the nonlinearity measures predicts low coverage.

Also, it is often the case that the most interesting parts of the functions to be estimated are the parts that are well determined according to LCA. If the correlation is valid, the curvature measure of (Bates and Watts, 1980) would be less suited to assess the validity of LCA predictions for the most interesting regions.

In this work, we seek to assess the validity of LCA for the model in (Sylte et al., 1999), with all parameters present, and with parameters associated with the lowest sensitivity decoupled from the analysis. The latter is done through use of curvature measures developed by (Cook and Goldberg, 1986), for subsets of parameters. We investigate how nonlinearities of the model affect the accuracy of confidence regions and intervals derived from LCA. We compare observed coverage to nonlinearity measures, both for the full parameter vector and for subsets of the parameters.

In Section 2, linearized covariance analysis and nonlinearity measures are discussed briefly. The PDE model studied in this paper is introduced in Section 3. In Section 4, some background on the correlation between nonlinearity, scale, and sensitivity is given. Numerical results of the investigation is presented in Section 5.

2 UNCERTAINTY ASSESSMENT

In many problems, the recovery of parameters, β, in some nonlinear model, $F(\beta)$, from measured values, Y, of the system being modeled, is central. The parameter estimates, β^*, are often found as the value of the parameters that minimizes a generalized least squares function

$$J(\beta) = (Y - F(\beta))^T \Sigma^{-1} (Y - F(\beta)), \tag{1}$$

where Σ is the covariance matrix of the measurement errors.

The accuracy issue may be investigated through synthetic cases where the true parameters are known. Model output using the true parameters, $\hat{\beta}$, may be added an error term, ε, from a given distribution, and the parameters corresponding to the minimum of $J(\beta)$ with $Y = F(\hat{\beta}) + \varepsilon$, may be calculated for a large number of different realizations of ε. This form of MC analysis will give accurate information on the probability distribution of the parameter estimates. The method is however computationally costly.

2.1 Linearized covariance analysis

LCA requires only the sensitivity matrix, A, of the model function at β^*. This information is likely to already have been computed during the minimization. The sensitivity matrix is used to construct an approximate covariance matrix for the parameters

$$P = (A^T \Sigma^{-1} A)^{-1}. \tag{2}$$

A $100(1-\alpha)\%$ confidence interval for a single parameter, when Σ is known, is given as

$$|\beta_j - \beta_j^*| \leq z_{1-\alpha/2} \sqrt{P_{jj}}, \tag{3}$$

where $z_{1-\alpha/2}$ is the upper $(1-\alpha/2)$ quantile for the Gaussian distribution.

Copyright © 1999 by ASME

In the PDE model studied in this work, the parameters enter the model as expansion coefficients of one or more functions $f(S,\beta) = \sum_i \beta_i \psi_i(S)$. It is of interest to find the confidence interval for the true value of the functions at particular values of the variable S. This confidence interval is given by all values f satisfying

$$|f - f^*| \leq z_{1-\alpha/2}\sqrt{\psi^T P \psi}, \tag{4}$$

where $f^* = f(S,\beta^*)$ is the estimated function value. The set of points $f \pm z_{1-\alpha/2}\sqrt{\psi^T P \psi}$ for all saturations is named pointwise confidence intervals for the function f.

Confidence regions for the parameter vector β when Σ is known, is in LCA approximated by

$$\left\{\beta \,\middle|\, (\beta-\beta^*)^T P^{-1}(\beta-\beta^*) \leq \chi^2_{p,1-\alpha}\right\}, \tag{5}$$

where $\chi^2_{p,1-\alpha}$ is the $(1-\alpha)$ quantile for the chi-square distribution with p degrees of freedom, and p is the number of parameters estimated.

Linearized $100(1-\alpha)\%$ confidence regions for parameter subsets may be given by (Seber and Wild, 1989)

$$\left\{\beta_2 | (\beta_2 - \beta^*{}_2)^T A_2^T (I_n - P_{A_1}) A_2 (\beta_2 - \beta^*{}_2) \leq \chi^2_{p_2,1-\alpha}\right\}. \tag{6}$$

In this equation, it is assumed that the parameter vector has been partitioned as $(\beta_1^T, \beta_2^T)^T$, with p_1 and p_2 elements, where β_2 is the interesting subset. The scaled sensitivity matrix, $\Sigma^{-1/2}A$, has likewise been partitioned into $[A_1, A_2]$, with p_1 and p_2 columns, and P_{A_1} is the projection operator into the subspace spanned by the columns of A_1.

2.2 Curvature measures

Let h be a unit vector in parameter space. Let $F_h = \sum_i h_i \partial F/\partial\beta_i$ be the first, and $F_{hh} = \sum_i \sum_j h_i h_j \partial F^2/\partial\beta_i\partial\beta_j$ the second order directional derivatives of the model function in the direction of h. The parameter effects, γ^t, and intrinsinc, γ^n, curvature measures of (Bates and Watts, 1980) are defined as

$$\gamma^t = \max_h \left\{\frac{\|F^t_{hh}\|}{\|F_h\|^2}\right\}, \quad \text{and} \quad \gamma^n = \max_h \left\{\frac{\|F^n_{hh}\|}{\|F_h\|^2}\right\}, \tag{7}$$

where the vector F_{hh} has been decomposed into F^t_{hh} parallel to the subspace spanned by F_h for all h, and F^n_{hh} normal to this space. Other decompositions have been used by other authors, e.g. in (Chavent and Liu, 1989). In (Cook and Goldberg, 1986), curvature measures for subsets of the parameters were developed.

2.3 Validation of predictions

Linearized covariance analysis gives statements about how the presence of measurement errors affects the probability of β^* being close to the true parameters $\hat{\beta}$. Curvature measures attempts to judge the quality of the LCA predictions.

Due to the complexity of the model, the accuracy of either prediction may only be tested by actually counting the percentage of times the LCA confidence regions or intervals contain the true parameters. This testing may be done using Monte Carlo simulations on a synthetic problem.

3 THE FORWARD MODEL

We study a macroscopic model for immiscible two-phase fluid flow in porous media. In porous media there exists, as the name indicates, an interconnected matrix of pores and channels through which fluids may flow. The fraction of space available for fluid flow is called the porosity, ϕ, and is an example of a volume averaged quantity, i.e., a quantity characteristic of a macroscopic point containing many individual pores. All quantities entering the model equations below should be interpreted in this sense. A standard reference on porous-media flow in the context of petroleum reservoirs is (Aziz and Settari, 1979).

To model single-phase flow, the permeability (i.e., the fluid conductivity), k, of the porous medium must be specified, as a function of the spatial coordinate. For two-phase flow, also the *relative permeability*, k_r, to each phase is needed. These quantities are introduced to account for the observed fact that the presence of one phase reduces the effective permeability of the other. Relative permeability to phase i is a function of the associated fluid saturation, S_i, i.e., the fraction of pore space occupied by phase i.

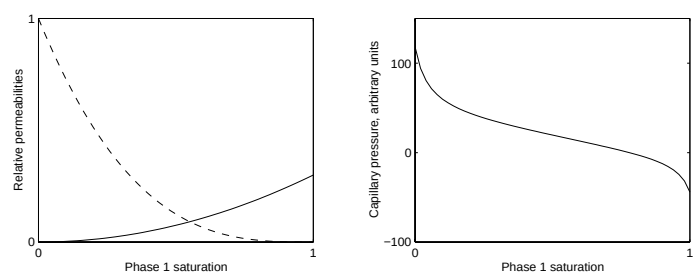

Figure 1. Typical flow functions. Left: Relative permeability functions (k_{r1} (solid), k_{r2} (dashed)), right: Capillary pressure function.

Due to interfacial tension, two phases may coexist in the porous medium at different phase pressures, p_i. The pressure difference is given by the *capillary pressure*, $P_c = p_2 - p_1$, which is a function of fluid saturation. With a nonzero P_c, the process

Copyright © 1999 by ASME

of fluid flow in porous media is not symmetrical with respect to the two phases.

The functions k_{r1}, k_{r2} and P_c are called flow functions. Since the k_{ri} are defined implicitly through the extension to two-phase flow, they may not be measured directly. The capillary pressure, P_c, may be measured, but physical considerations make it advantageous to estimate it together with the k_{ri}, see, e.g., (Kulkarni et al., 1998). The flow functions are monotonic in S_1, typical examples are given in Figure 1. In the numerical experiments in Chapter 5, the flow functions are represented as third-order B-spline expansions.

In the model used in this work, we assume constant densities and viscosities (μ_i) of the phases, and constant porosity and permeability of the porous medium. Furthermore, we study one-dimensional flow in the horizontal direction. This leads to

$$\phi\frac{\partial S_i}{\partial t} = \frac{\partial}{\partial x}\left(\frac{k k_{ri}(S_1)}{\mu_i}\frac{\partial p_i}{\partial x}\right), \quad i = 1,2, \tag{8}$$

$$p_2 - p_1 = P_c(S_1), \tag{9}$$

$$S_1 + S_2 = 1. \tag{10}$$

The solution of these equations for given boundary conditions constitutes the forward model used in this work.

This type of model is widely applied in predictive calculations of fluid flow in large-scale petroleum or ground water reservoirs. Prior to a successful application of the model, the flow functions need to be specified. To this end, laboratory experiments are performed, where fluids are driven through small samples of the porous medium with an applied pressure drop, and the flow functions are determined by solving the inverse problem associated with the measured data and the above flow model, see e.g., (Kulkarni et al., 1998; Sylte et al., 1999). Typically, one collects data on the fluid production and the pressure drop across the core sample.

In these experiments, it is difficult to gather information close to initial saturation of the displaced fluid, and the corresponding regions of the flow functions will usually not be accurately determined. This corresponds to some parameter combinations having associated low sensitivity.

4 NONLINEARITY, SCALE, AND SENSITIVITY FOR GENERIC MODELS

In this section, we give a brief background on, and present some results illustrating, a correlation between nonlinearity, scale, and sensitivity, for a certain class of models. It is included primarily as a motivation for the remaining sections in the paper. Readers who are particularly interested in the correlation as such, will find a more thorough description in (Grimstad and Mannseth, 1999).

4.1 Model classes

Suppose that the task is to estimate the parameters, β, associated with the function $f(x,\beta)$ from measured data on some nonlinear function of f. In (Grimstad and Mannseth, 1999), the following model classes are studied:

$$m(x,\beta) = g(f(x,\beta)), \tag{11}$$

for models in the non-integrated class, and

$$M(x,\beta) = \int_0^x m(t,\beta)\,dt, \tag{12}$$

for the class of integrated models. The function g can be any smooth nonlinear function. Note that recovery of a coefficient function, f, in an ODE- or a PDE-model have strong similarities to the latter class, since solutions to such model equations are in some sense integrals involving a nonlinear function of f.

4.1.1 Model derivatives

For the calculation of sensitivity and curvature of the models, the first- and second-order directional derivatives in an arbitrary direction h are needed. If the function f is parameterized by a linear expansion in a set of basis functions, $f(x,\beta) = \sum_i \beta_i \psi_i(x)$, these are

$$m_h(x,\beta) = \sum_i h_i \frac{\partial m(x,\beta)}{\partial \beta_i} = g'(f(x,\beta))\,f(x,h), \tag{13}$$

$$m_{hh}(x,\beta) = \sum_{i,j} h_i h_j \frac{\partial^2 m(x,\beta)}{\partial \beta_i \partial \beta_j} = g''(f(x,\beta))\,f^2(x,h). \tag{14}$$

for the non-integrated models. The derivatives of any integrated model, M, are obtained by integrating Equations 13, 14 with respect to x.

4.1.2 Sensitivity and curvature

We want to investigate if there is a general correlation between low sensitivity and large curvature seen only within the class of integrated models. This means that we look for reasons causing $||M_h||$ to be small and $||M_{hh}||/||M_h||^2$ to be large, that would not produce similar effects in $||m_h||$ and $||m_{hh}||/||m_h||^2$.

Suppose that h is the direction vector of maximum curvature for a model. There is one possibility that h is also a direction of low sensitivity which is a unique feature of integral models: If the integrand is oscillating rapidly about zero as a function of the integration variable. From Equations 13, 14, it is seen that if $g'(f(x,\beta))$ is slowly varying, such that rapid oscillations in m_h are caused only by rapid oscillations in $f(x,h)$, similar oscillations in m_{hh} would not occur. This would have the desired influence on the sensitivities and curvatures in both model classes, indicating the existence of a correlation between high nonlinearity,

Copyright © 1999 by ASME

low sensitivity, and small scale (in the sense of rapid oscillations) for the class of integrated models. In (Grimstad and Mannseth, 1999), several other scenarios leading to rapid oscillations of the integrand are discussed.

4.2 Results for generic models

To check the predictions of the theory, numerical experiments with the selection of nonlinear model functions listed in Table 1, have been performed. Also, several normalized multi-scale expansion bases for $f(x,h)$ were tested, offering a variety of possibilities to generate both slowly varying and rapidly oscillating functions. See (Grimstad and Mannseth, 1999) for details.

Table 1. Nonlinear model functions.

A:	$g(f) = f + \exp(f)$
B:	$g(f) = f/(1+f^2)$
C:	$g(f) = f^2/2$
D:	$g(f) = 1/2\ln(1+f^2)$
E:	$g(f) = 2\exp(f+1) - \exp(2f-3)$
F:	$g(f) = 1 + \exp(-f^2/5)$
G:	$g(f) = [1+\exp(-f^2/5)]^{1/2}$
H:	$g(f) = (f+5)^{f/5}$

Fig. 2 shows the curvature, γ^t, and the norm of the sensitivity vector in the unit parameter directions when combining the model functions G and H in Table 1 with a basis of five sine-functions with half-periods ranging from 1 to $2.5 \cdot 10^{-2}$. The parameters are ordered according to half-period lengths of the associated basis functions, such that parameter no. 1 corresponds to half-period 1, and parameter no. 5 corresponds to half-period $2.5 \cdot 10^{-2}$. The function $f(x,\beta)$ is proportional to the sine-function with half-period 1, i.e., a slowly varying function on [0,1].

All choices for $g(f)$, also those not shown here (Grimstad and Mannseth, 1999), follow the same trend in behavior: For the integrated models, perturbations $f(x,h)$ with shorter characteristic length have associated a lower sensitivity and a higher curvature. For the non-integrated models, the variation in sensitivity and curvature is minor and difficult to relate to the characteristic length of $f(x,h)$.

In (Grimstad and Mannseth, 1999), several other scenarios were considered, and among other things, it was found that the correlation is less evident if $f(x,\beta)$ is not slowly varying. Also, it

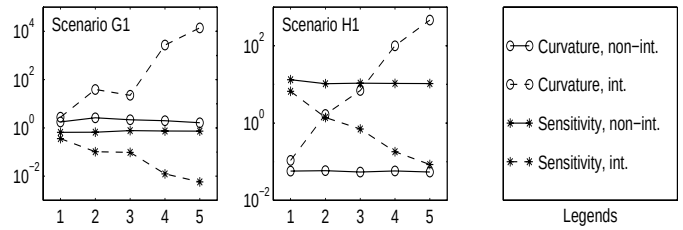

Figure 2. Correlation between nonlinearity (curvature), scale, and sensitivity. Scale decreases from left to right.

was shown that results for the class of integrated models, Equation 12, holds for the solution to an ODE model considered in (Chavent and Liu, 1989; Liu, 1993). That solution can be explicitly expressed as an integral in x (Liu, 1993), but is more complex than Equation 12.

4.2.1 Relation to the current forward model

An estimated function in the current forward model, Equations 8-10, is a not a direct function of the integration variable, as is the case for the models described by Equation 12 and the model in (Chavent and Liu, 1989; Liu, 1993). Rather, it is a function of x and t through the dependence on fluid saturation. To study this kind of dependence, Equation 12 should perhaps be replaced by generic models of the form

$$M(t,\beta) = \int_0^t \int_0^L g(f(S(u,v),\beta))\, du\, dv. \tag{15}$$

An explicit correspondence between such a model and Equations 8-10 is not known. Hence, Equation 15 is only intended as an indication as to how the PDE-model, Equations 8-10, might be related to the class of models where a correlation between nonlinearity, scale, and sensitivity exists. However, an important prerequisite for a strong correlation is fulfilled; relative permeability and capillary pressure are known to be slowly varying functions of saturation, see e.g. Figure 1.

5 NUMERICAL EXPERIMENTS

We want to see if the curvature measures of (Bates and Watts, 1980) may be calibrated for consistent use with the reservoir fluid flow model. As noted, the results of (Sylte et al., 1999) seemed to be in conflict with the results of (Donaldson and Schnabel, 1987). The synthetic cases used in this work is based on one of the cases studied in (Sylte et al., 1999). The total number of parameters in the experiments vary between 10 and 28, see also Table 2. A detailed description of the setup of the cases is found in (Grimstad et al., 1999).

Copyright © 1999 by ASME

The distribution of the sets of MC-estimated parameters is compared with predictions from LCA at the true parameter value $\hat{\beta}$. If these predictions are correct, the percentage of estimates contained within the confidence regions/intervals should be close to the nominal level.

Further, we calculate the maximum curvature measures, γ^t and γ^n, of (Bates and Watts, 1980), to see if these measures correlate well with the quality of the LCA predictions.

Finally, we identify the parameters with least sensitivity in each case, and calculate the coverage of subset confidence regions for several subsets of the parameters when the least sensitive parameters are excluded. The coverage of these regions are compared to the subset curvature measure of (Cook and Goldberg, 1986).

5.1 Results with full parameter vector

Table 2 lists the values of maximum curvature calculated for the cases, and the observed coverage for 95% linearized confidence regions. PE denotes the *parameter effects* curvature, and IN denotes the *intrinsic* curvature. The maximum curvature values have been normalized by the appropriate critical value suggested by (Bates and Watts, 1980). This means that curvature values above one are above the critical value. We note that all the calculated PE values are above the recommended cutoff values, by at least one order of magnitude.

We also note that the degree of coverage does not seem to be particularly well correlated with the maximum curvature measure. The coverage for the 95% level is seen to vary between 80 and 88%, and is higher for case I1 than for cases I1a and I1b, in spite of considerably higher curvature in the former case.

If the results of (Donaldson and Schnabel, 1987) carried over to the reservoir model, curvature measures as high as these would imply a degree of coverage for LCA confidence regions well below the nominal level. In particular, with curvatures as high as for I1, the observed coverage could be expected to be below 20% for a 95% confidence region. A scaled curvature of above 20, as for the other cases, would imply coverage between 40 and 80%. None of the cases studied displays observed coverage below 80% for the 95% confidence level. Thus, the coverage is clearly higher than expected from the results of (Donaldson and Schnabel, 1987).

Table 2. Scaled maximum curvatures and observed coverage for 95% confidence regions for the cases studied.

Case	Scaled max. curv.		Estimated	Observed
	PE	IN	functions	coverage
I1	$5.7 \cdot 10^4$	$5.1 \cdot 10^3$	$P_c + k_r$	87%
I1a	$2.4 \cdot 10^1$	$6.9 \cdot 10^0$	k_r	82%
I1b	$2.6 \cdot 10^1$	$4.7 \cdot 10^0$	P_c	80%
I2	$2.7 \cdot 10^1$	$4.3 \cdot 10^1$	P_c	88%

We select case I1b for further illustrations of some effects seen in all the cases. More illustrations are found in (Grimstad et al., 1999).

Figure 3 illustrate coverage of confidence regions (left) and pointwise confidence intervals (right). Left, the distance from the estimated parameters to the true parameters is plotted. The distance is normalized by the LCA inverse covariance matrix at $\hat{\beta}$, i.e., we calculate $(\beta^* - \hat{\beta})^T P^{-1} (\beta^* - \hat{\beta})$ for each estimation. When the resulting values are sorted, the observed coverage of 50, 75 and 95% confidence regions may be read off as the fraction of the estimates with normalized distance less than the appropriate cutoff levels, given as horizontal lines.

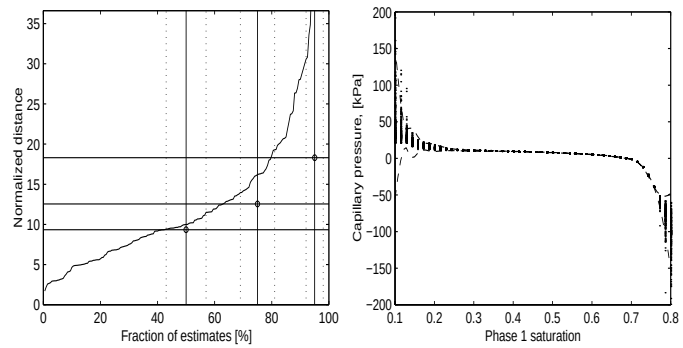

Figure 3. Left: Distribution of normalized distance from true to estimated parameters. Cutoff values for 50, 75 and 95% confidence regions (horizontal lines), 95% confidence intervals for the expected coverage (vertical dotted lines). Right: Estimated capillary pressure from MC analysis (dotted curves), and linearized confidence intervals (dashed curves)

The expected coverage for exact regions is statistically distributed, and the 95% confidence intervals for the expected coverage, for these confidence levels and the number of estimations done, is given by the dotted vertical lines in the figure.

We note that the coverage is closer to the nominal level for the 50 and 75% confidence regions than for the 95% regions. This behavior was also observed for the models studied in (Donaldson and Schnabel, 1987).

In (Donaldson and Schnabel, 1987), the correlation between LCA confidence intervals and curvature is not reported, but general considerations suggests that the minimum observed coverage for intervals should be higher than for regions, since more points in parameter space are included when correlations between parameters are neglected. This was also observed. For the cases studied here, the minimum observed coverage for con-

Copyright © 1999 by ASME

fidence intervals was generally above nominal coverage, and never below 90% for the 95% level.

Since it is the flow *functions* that are the interesting estimated quantities, the uncertainty in the estimates are most conveniently plotted as pointwise confidence intervals about these functions. The estimated capillary pressure from the MC analysis in case I1b, together with the pointwise confidence intervals, is shown to the right on Figure 3. As for the other cases, the observed coverage for pointwise confidence intervals is above the nominal level, in spite of the high curvature measures.

From these results, it seems that, for the current model, the nonlinearity measure of Bates and Watts may not be used consistently to indicate coverage far below nominal for linearized confidence regions. Neither do high values of the curvature measures imply coverage below nominal for pointwise confidence intervals, even when the curvature measure is several orders of magnitude above the critical levels.

If the current model belongs to the class of models for which a correlation between high nonlinearity and low sensitivity exists (see Section 4), large spread in the MC estimates will coincide with wide LCA regions/intervals, explaining the above observations. Figure 4 shows a clear correlation for case I1b. To the left, the sensitivity and PE curvature in the unit parameter directions are shown. Note that the curvature values are not the highest possible for this case, since this would require a linear combination of several parameters. The directions of maximum curvature and least sensitivity coincide with high accuracy, as seen to the right on Figure 4.

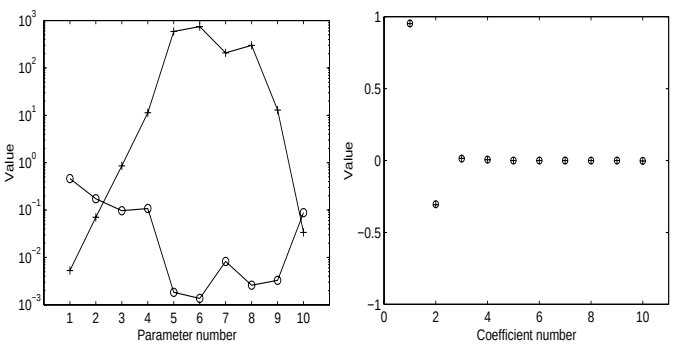

Figure 4. Curvature (∘) and sensitivity (+) for individual parameters (left). Directions of maximum curvature and minimum sensitivity (right).

Since it seems like high curvature is connected to parameters with low sensitivity, we want to investigate into whether curvature measures may be used more consistently if we remove from the analysis the parameters with the lowest sensitivity, and calculate curvature measures and confidence regions for the remaining subsets. Moreover, this will enable us to assess the validity of LCA for parameters where LCA indicate high accuracy.

5.2 Results with subsets of the parameters

The curvature measure for parameter subsets developed in (Cook and Goldberg, 1986) is used to study the parameter subsets chosen. This measure requires only a relatively small amount of computations once the curvature array for the full parameter vector has been computed.

When the parameters causing high curvature are excluded, we expect that the subset curvature measure should correspond better with the degree of agreement between LCA and observed coverage. Specifically, if the measure proves to be useful, the agreement between LCA and observed coverage should be consistently good for values of the curvature measure below some critical value, preferably the value suggested in (Cook and Goldberg, 1986).

Because of the correlation shown in Figure 4, the parameters to be excluded should be the parameters with least sensitivity. Figure 4 may be used to identifiy those. Another method is also possible. Since the flow function representation utilized (B-splines) have basis functions with local support, the parameters with least sensitivity may also be identified in plots of the pointwise confidence intervals (see, right plot on Figure 3). Note that this gives additional information on the sensitivity in cases where the scaling of the parameters is different between the flow functions. These methods have been validated in (Grimstad et al., 1999).

Using the proposed method of excluding parameters, we examine some subsets for each of the cases, generally aiming at excluding as few parameters as possible.

Table 3 gives the subsets examined and the calculated subset curvatures. The curvatures have been scaled by the critical value suggested by (Cook and Goldberg, 1986). Also given are the observed coverage for 95% subset confidence regions. Note that in all cases, the curvature measure is reduced from the maximum level. Accordingly, the coverage for all subset cases have increased compared to the full parameter vector cases — compare Tables 2 and 3.

The coverages for these subsets are inside, or slightly outside, the 95% confidence intervals about the expected coverage for the 95% confidence regions. Also, the subset coverage is at or above the nominal level for subset curvatures significantly above the cutoff value proposed in (Cook and Goldberg, 1986). The coverage is generally on the conservative side if we remove parameters having the largest coefficients in the vector of least sensitivity. The subset curvature for such subsets is seen to be significantly reduced from the maximum curvature.

To further illustrate, Figure 5 shows the distribution of normalized distance from the true parameters for the subsets of case I1b in Table 3. A comparison with corresponding results for the

Copyright © 1999 by ASME

Table 3. Parameter subsets studied, with subset curvature measures and observed coverage for 95% subset confidence regions.

Case	Subset k_{r1}	Subset k_{r2}	Subset P_c	Subset curvature	Observed coverage
I1	1–8,	12–16,	20–25	$3.6 \cdot 10^3$	99%
	1–8,	9–16,	20–25	$4.5 \cdot 10^3$	98%
	1–8,	9–16,	21–24	$4.2 \cdot 10^3$	97%
I1a	1–8,	12–16		$1.3 \cdot 10^1$	97%
	1–8,	13–16		$1.2 \cdot 10^1$	96%
	5–8,	13–16		$2.2 \cdot 10^0$	100%
	6–8,	14–16		$4.1 \cdot 10^{-1}$	97%
I1b			3–10	$3.7 \cdot 10^0$	93%
			3–9	$3.0 \cdot 10^0$	99%
I2			3–10	$1.4 \cdot 10^1$	98%

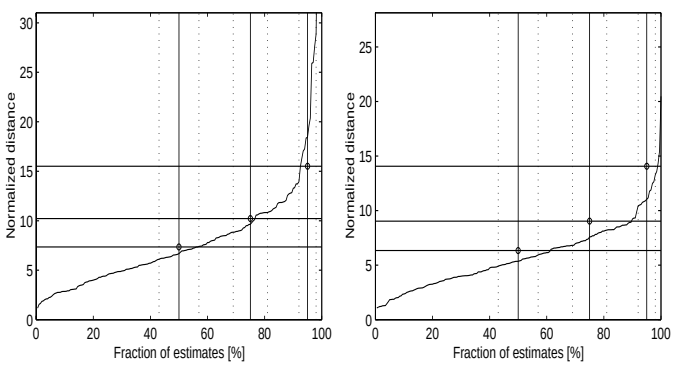

Figure 5. Observed coverage for subset confidence regions. Subset 3–10 (left) and 3–9 (right).

full parameter vector (see, Figure 3, left) illustrates the results found in Table 3.

Since the representation for the flow functions utilizes a basis with local support, it is possible to associate the parameters removed from the analysis with parts of the flow functions. The parameters removed are associated with saturation regions for which the flow functions are not well determined (the parameters have small sensitivities, and, hence, large confidence intervals result). The remaining parameters are associated with saturation intervals where the flow functions have narrower confidence intervals. This work suggests that the pointwise confidence intervals in these saturation regions seem to be accurate and conservative.

6 SUMMARY AND CONCLUSIONS

The validity of linearized confidence regions and intervals for a porous-media flow model have been assessed.

It is found that the quality of linearized covariance analysis is not directly related to curvature measures of nonlinearity for the full parameter vector. The reason may be that the current model belongs to a class displaying a strong correlation between low sensitivity and high curvature.

We observe maximum curvature well above previously proposed critical values, but coverages for confidence regions never far below the nominal level. The coverage of pointwise confidence intervals was generally above the nominal level.

When excluding parameters of lowest sensitivity from the nonlinearity analysis, it is found that the coverage of linearized subset confidence regions is consistently good. It is also found that the coverage is at or slightly above the nominal level when the subset curvature is significantly lower than the maximum curvature for the full parameter vector.

This work suggests that the LCA pointwise confidence intervals for the parts of the flow functions that are well determined, are accurate and conservative.

REFERENCES

K. Aziz, and A. Settari, *Petroleum Reservoir Simulation*, Applied Science Publishers, London, (1979).

D. M. Bates and D. G. Watts, Relative curvature measures of nonlinearity, Journal of the Royal Statistical Society, ser. B, 42(1):1–25, (1980).

G. Chavent and J. Liu, Multiscale parametrization for the estimation of a diffusion coefficient in elliptic and parabolic problems, in *Fifth IFAC Symposium on Control of Distributed Parameter Systems, Perpignan, France*, June (1989).

R. Cook and M. L. Goldberg, Curvatures for parameter subsets in nonlinear regression, The Annals of Statistics, 14(4):1399–1418, (1986).

J. R. Donaldson and R. B. Schnabel, Computational experience with confidence regions and confidence intervals for nonlinear least squares, Technometrics, 29(1):67–82, (1987).

A.-A. Grimstad, K. Kolltveit, T. Mannseth, and J.-E. Nordtvedt, Validation of linearized covariance analysis for a porous-media flow model, Submitted (1999).

A.-A. Grimstad and T. Mannseth, Nonlinearity, scale, and sensitivity for parameter estimation problems, Submitted (1999).

R. Kulkarni, A.T. Watson, J.-E. Nordtvedt, and A. Sylte, Two-phase flow in porous media: Property identification and model validation, AIChE Journal, 44(11):2337–2350, (1998).

J. Liu, A multiresolution method for distributed parameter estimation, SIAM Journal on Scientific Computing, 14(2):389–405, (1993).

G. A. F. Seber and C. J. Wild, *Nonlinear Regression*, John Wiley & Sons, New York, (1989).

A. Sylte, E. Ebeltoft, A.-A. Grimstad, R. Kulkarni, J.-E. Nordtvedt, and A. T. Watson, Design of two-phase flooding experiments, Submitted (1999).

Copyright © 1999 by ASME